

Synthesis, characterisation, and evaluation of stable, efficient modified nanocopper-based glycerol hydrogenolysis catalysts

Zhiguo Lv , Zhipeng Xie, Zhenmei Guo, Xia Liu, Pei Liu

School of Chemical Engineering, Qingdao University of Science and Technology, Qingdao 266042, People's Republic of China

✉ E-mail: lvzhiguo@qust.edu.cn

Published in Micro & Nano Letters; Received on 5th November 2016; Revised on 17th January 2017; Accepted on 27th January 2017

A series of CuO/SiO₂ catalysts containing different modifiers were prepared via co-precipitation and used for glycerol hydrogenolysis. CuO–CeO₂/SiO₂ gave the best glycerol conversion rate (100%) and highest selectivity for 1,2-propanediol (up to 95%). Reactions were carried out under the following conditions: temperature, 220°C; H₂ pressure, 0.5 MPa; glycerol concentration, 100 wt.%; and H₂/glycerol molar ratio, 35:1. The catalysts were characterised by X-ray diffraction, NH₃ temperature-programmed desorption, N₂ adsorption, and scanning electron microscopy. The CuO–CeO₂/SiO₂ catalyst had smaller particle sizes, better dispersion, and greater specific surface area than the CuO/SiO₂, CuO–phosphotungstic acid (PTA)/SiO₂, and CuO–CeO₂–PTA/SiO₂ catalysts.

1. Introduction: In the foreseeable future, base oil, which is an unsustainable fuel from environmental, economic, and societal perspectives, will gradually lose its dominance in the global energy supply. Many national governments have introduced targeted policies to reduce fossil fuel usage, and are employing a broadening range of biological resources as fuel [1, 2]. The production of biodiesel fuels from renewable biomass resources is particularly attractive [3]. Owing to the rapid development of biodiesel production, large quantities of glycerol are formed as a by-product. Around 1 kg of glycerol is produced for every 10 kg of biodiesel manufactured, resulting in supplies of glycerol exceeding demand [4]. With the increasing availability of cheap glycerol, new industries utilising glycerol will develop rapidly. Glycerol is a promising feedstock in the production of a wide range of value-added chemicals. Propanediol (PDO) synthesis from glycerol has attracted significant interest. In the past few years, a large number of studies on the reactions of glycerol have been reported. Under suitable hydrogen pressure, glycerol hydrogenolysis, affording 1,2- and 1,3-PDOs, has been reported in the presence of supported Cu [5–10], Ru [11–13], Rh [14–16], Pt [17, 18], Co [19, 20], Re [21], Ni [22], and Ag [23] catalysts. Noble metals such as Ru, Rh, and Pt are well known to activate hydrogen molecules and are widely employed as hydrogenation catalysts, but are extremely expensive and sometimes have lower activities than Cu-based catalysts. Compared with noble metal catalysts, highly dispersed Cu-based catalysts have higher activities, selectivities, and stabilities for the catalytic hydrogenolysis of glycerol to PDOs, which lends them a bright prospect in future industrial production.

In this Letter, we report the synthesis of 1,2-PDO from glycerol with high selectivity over supported CeO₂-modified nanocopper-based catalysts under suitable hydrogen pressure.

2. Experimental Result

2.1. Catalyst preparation: A series of copper-based catalysts were prepared via co-precipitation. The preparation of CuO–CeO₂/SiO₂ is described here as an example. Calculated amounts of Cu (NO₃)₂·3H₂O (analytical reagent (AR), Tianjin Badische Anilin-und-Soda-Fabrik (BASF), China) and NaOH (AR, Tianjin Bodi Chemical Co., Ltd., China) were separately dissolved in distilled water under stirring to prepare 35 and 16 wt.% solutions, respectively. These two solutions were added slowly into a three-necked flask under vigorous stirring at 45°C, with the pH maintained at 12 via controlling the dropping speed. Next, an

amount of Ce(NO₃)₃·6H₂O ($m(\text{CuO}):m(\text{CeO}_2)=6:1$) dissolved in distilled water was added to the reaction mixture. Finally, silica sol for industrial use (Qingdao Haiyang Chemical Co., Ltd., China) was added to the precipitation system. The resulting suspension was then aged at 85°C for 6 h under stirring, and then filtered and washed with distilled water. The precipitates were dried overnight and calcined for 6 h at 500°C in air to obtain the final catalyst.

2.2. Catalyst characterisation: X-ray diffraction (XRD) patterns of the powdered catalysts were recorded on an X-ray diffractometer (D-MAX2500-PC, Rigaku Corp.) using CuK α radiation ($\lambda=1.5418$ Å) in the range $2\theta=5$ –85°, at a scanning speed of 5°/min. Used catalysts were reprocessed before XRD analysis by cooling to room temperature in N₂ flow (180 sccm) and collecting under Ar.

Temperature-programmed desorption (TPD) analyses were carried out on a Micromeritics AutoChem II instrument to detect the acidity of these modified catalysts. Prepared samples were reduced under a mixed flow of H₂ and N₂ (1:9, v/v) at 320°C for 2 h, and then cooled to room temperature under pure He. A mixed stream of 10% NH₃/He was introduced at room temperature to allow NH₃ adsorption for 30 min, before purging the reactor with He at 100°C for 2 h to remove physically adsorbed NH₃. TPD measurements were conducted under He flow from room temperature to 500°C with a heating rate of 5°C min^{–1}. NH₃ evolution was recorded and monitored by a thermal conductivity detector.

Brunauer–Emmett–Teller (BET) surface areas, pore volumes, and distribution were calculated from the adsorption branches of N₂ adsorption isotherms using the Barrett–Joyner–Halenda model on a Micromeritics ASAP2400 apparatus.

Scanning electron microscopy (SEM) images of the catalysts were obtained using a field emission SE microscope (JEOL-6700F, Japan Electron Co., Ltd.), conducted at an accelerating voltage of 10 kV.

2.3. Catalytic activity test: The fixed bed reactor (East China University of Science and Technology, China) employed a 1/200 diameter tube with a working bed volume of 25 ml. Abraded catalysts were put into the tube and covered with granulated quartz sand on both sides. Before testing, the catalysts were reduced using a mixture of H₂ and N₂ with flows of 30 and 170 ml/min, respectively, under 1.5 MPa H₂ pressure and 2.0 MPa N₂ pressure with temperature programme from room temperature to 250°C in the fixed bed reactor overnight. Glycerol aqueous

solution was transported into the reactor via a micropump, and H₂ was provided by high-pressure cylinders, with H₂ flow controlled by a gas-flow controller. Reaction temperature, H₂ pressure, and H₂ flow were altered to optimise the reaction conditions. Products were collected in cooled traps for online analysis. In particular, some reactions proceeded under the following conditions: temperature, 220°C; H₂ pressure, 0.5 MPa; H₂/glycerol molar ratio, 35:1; and 100 wt.% glycerol aqueous solution.

Quantitative product analysis was conducted using a GC-122 chromatograph equipped with a flame ionisation detector and capillary column (SE-30, 30 m length, 0.25 mm i.d., and 0.25 µm film thickness). Results were corrected using the area normalisation method, and quality analysis was obtained via gas chromatography–mass spectrometry (GC–MS; Agilent 7890A-5975C) with a P-5 capillary column (50 m length, 0.25 mm i.d., and 0.25 µm film thickness).

3. Results and discussion

3.1. Catalyst characterisation: The crystalline structures of the prepared nanocopper-based catalysts [CuO/SiO₂, CuO–phosphotungstic acid (PTA)/SiO₂, CuO–CeO₂–PTA/SiO₂, and CuO–CeO₂/SiO₂] were investigated by XRD. XRD patterns of the calcined copper-based catalysts are shown in Fig. 1. Characteristic peaks at $2\theta = 35.7^\circ$, 38.8° , and 48.6° , corresponding to the CuO structure, were detected for all catalysts. The CuO characteristic peaks for the CuO–CeO₂/SiO₂ catalyst were less sharp than for the others, indicating that CuO–CeO₂/SiO₂ had a smaller average particle size. When a small amount of CeO₂ was added to the copper-based catalyst, characteristic CeO₂ peaks were not clearly visible via XRD analysis, indicating that CeO₂ was highly dispersed in the CuO–CeO₂/SiO₂ catalyst.

After the hydrogenolysis reaction, the catalysts were again characterised by XRD (Fig. 2). The characteristic CuO peaks disappeared in CuO–PTA/SiO₂, CuO–CeO₂–PTA/SiO₂, and CuO–CeO₂/SiO₂ catalysts, with new characteristic peaks appearing at $2\theta = 43.3^\circ$, 50.4° , and 74.2° , corresponding to Cu⁰. However, for the used CuO/SiO₂ catalyst, the characteristic CuO peaks remained intact, indicating that the catalyst was easily oxidised. Characteristic peaks at $2\theta = 26.6^\circ$ and 68.8° , corresponding to SiO₂, appeared for CuO–CeO₂/SiO₂. We speculated that some quartz sand was present in the used catalyst, and that some formless silica gel had become a crystalline polymer in the presence of catalyst. CeO₂ contributed to the CuO dispersion in the CuO–CeO₂/SiO₂ catalyst, resulting in the

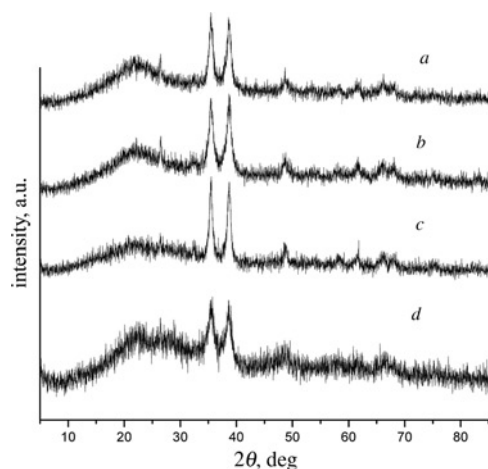


Fig. 1 XRD patterns of calcined catalysts

a CuO/SiO₂
b CuO–PTA/SiO₂
c CuO–CeO₂–PTA/SiO₂
d CuO–CeO₂/SiO₂

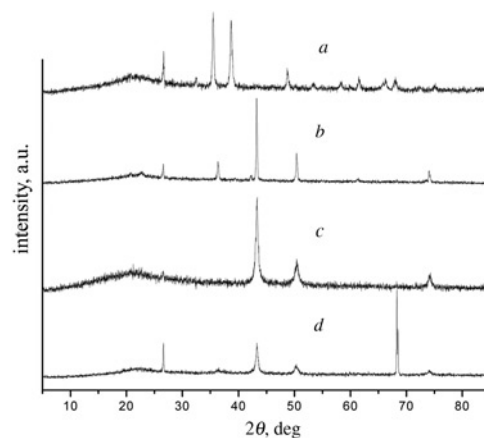


Fig. 2 XRD patterns of used catalysts

a CuO/SiO₂
b CuO–PTA/SiO₂
c CuO–CeO₂–PTA/SiO₂
d CuO–CeO₂/SiO₂

characteristic CuO peaks being less sharp for CuO–CeO₂/SiO₂ than the other catalysts, demonstrating that CuO–CeO₂/SiO₂ had smaller particle sizes and better dispersion.

The acidities of the modified catalysts, as determined by NH₃-TPD, are shown in Fig. 3. Between 40 and 500°C, two NH₃ desorption peaks were detected, indicating that two different acid sites were present in these catalysts. The relative areas of desorbed NH₃ were calculated (see Table 1). In the temperature ranges 45–205 and 205–415°C, weak and medium acid sites were identified

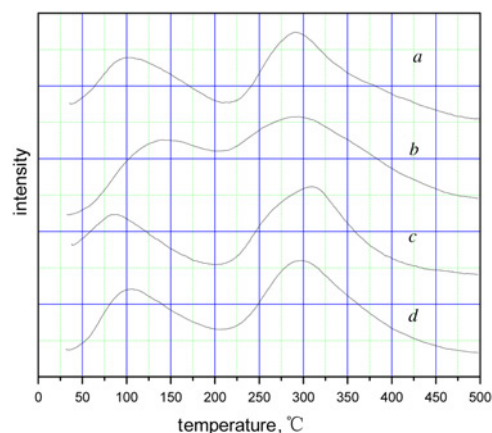


Fig. 3 NH₃-TPD profiles of copper-based catalysts

a CuO/SiO₂
b CuO–PTA/SiO₂
c CuO–CeO₂–PTA/SiO₂
d CuO–CeO₂/SiO₂

Table 1 NH₃-TPD results for copper-based catalysts

Catalyst	Relative total area of NH ₃ desorbed	NH ₃ desorbed region (relative area)	
		ca. 45–205°C	ca. 205–415°C
CuO/SiO ₂	4.5128	1.7355	2.7773
CuO–PTA/SiO ₂	12.8006	4.7202	8.0804
CuO–CeO ₂ –PTA/SiO ₂	10.9781	4.3223	6.6558
CuO–CeO ₂ /SiO ₂	10.0529	3.4971	6.5558

Table 2 Physical properties of copper-based catalysts

Catalysts	Specific surface area, m ² /g	Pore volume, cm ³ /g	Pore diameter, nm
CuO–CeO ₂ /SiO ₂	128.4	0.62	19.33
CuO/SiO ₂	42.9	0.30	34.47
CuO–PTA–CeO ₂ /SiO ₂	89.1	0.53	22.75
CuO–PTA/SiO ₂	55.9	0.34	24.57

from desorption peaks. The relative area of desorbed NH₃ detected on CuO/SiO₂ was less than that of the other catalysts. In contrast, when PTA and CeO₂ were added to the catalyst, the amount of weak and medium acid sites was greatly enhanced. Compared with CuO–CeO₂/SiO₂, CuO–CeO₂–PTA/SiO₂ had a slightly larger relative area of desorbed NH₃. In combination, this data confirmed that catalyst activity was associated with the amount of acid sites. Too many acid sites would trigger other side reactions and decrease selectivity for the target products, whereas too few acid sites would result in no reaction at all.

BET surface areas, pore volumes, and average pore diameters were calculated from adsorption isotherms of each modified catalyst (see Table 2). The specific surface areas and pore volumes of CuO–PTA/SiO₂ and CuO–CeO₂/SiO₂ increased rapidly with the addition of PTA and CeO₂, respectively, whereas their average pore diameters decreased. Adding PTA and CeO₂ together, as in CuO–CeO₂–PTA/SiO₂, resulted in decreased BET surface area and pore volume and increased average pore size compared with CuO–CeO₂/SiO₂. Therefore, when only CeO₂ was added to CuO/SiO₂, the specific surface area and pore volume of the copper-based catalysts increased and the pore diameter decreased significantly, resulting in better catalytic activity.

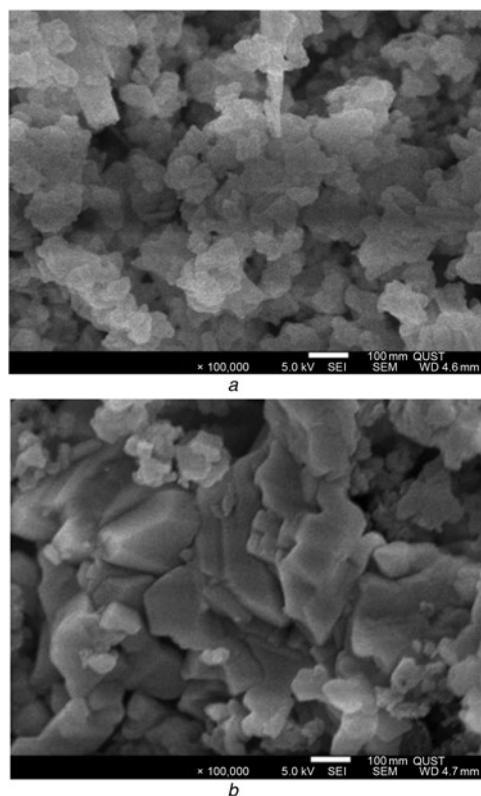


Fig. 4 SEM images of CuO/SiO₂ hydrogenation catalyst
a Before reaction
b After reaction

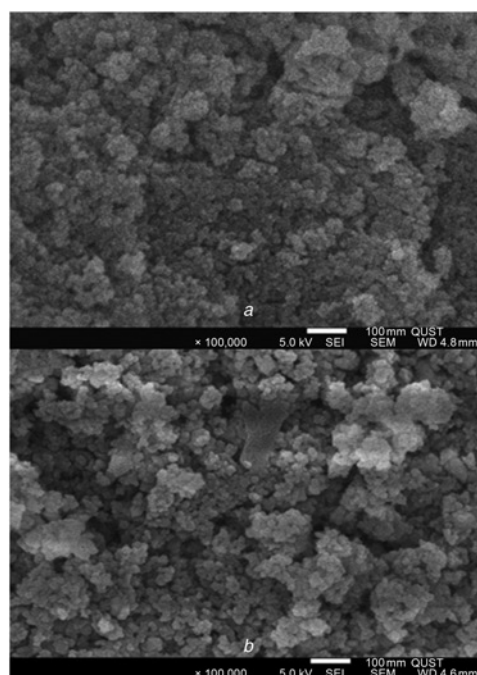


Fig. 5 SEM images of CuO–CeO₂/SiO₂ hydrogenation catalyst
a Before reaction
b After reaction

Catalyst morphologies were observed by SEM, as shown in Figs. 4 and 5. SEM imaging showed that CuO/SiO₂ catalyst particles were well organised and dispersed before the reaction with excellent resolution (Fig. 4a). However, after the reaction, the catalyst particles were more aggregated, exhibiting smaller clearances, larger sizes, and uneven dispersion, indicating a certain degree of sintering and a slightly altered catalyst morphology. Fig. 5 shows that there was no significant change in the morphology of the modified CuO–CeO₂/SiO₂ catalyst during or after the reaction. Comparing Figs. 4 and 5, we can see that the stability of the CuO–CeO₂/SiO₂ catalyst was better than that of CuO/SiO₂, and thus would be expected to have a longer operating lifetime.

3.2. Catalytic reaction: The catalytic performances of the as-prepared catalysts in the hydrogenolysis of glycerol to 1,2-PDO are shown in Fig. 6. CuO–CeO₂/SiO₂ showed the best catalytic activity for the hydrogenolysis, giving a 100% conversion and 95.47% selectivity for 1,2-PDO. Owing to their

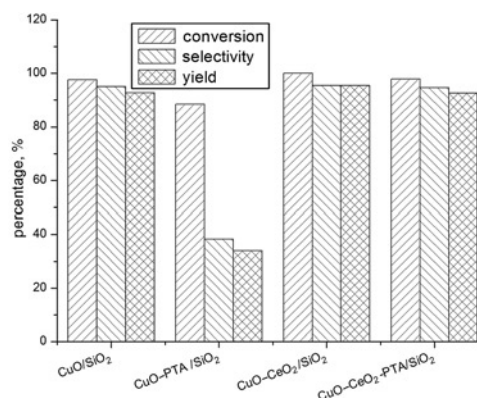


Fig. 6 Catalytic performance of copper-based catalysts in the hydrogenolysis of glycerol to 1,2-PDO. Reaction conditions: temperature, 220°C; H₂ pressure, 0.5 MPa; glycerol concentration, 100%; and H₂/glycerol molar ratio, 35:1

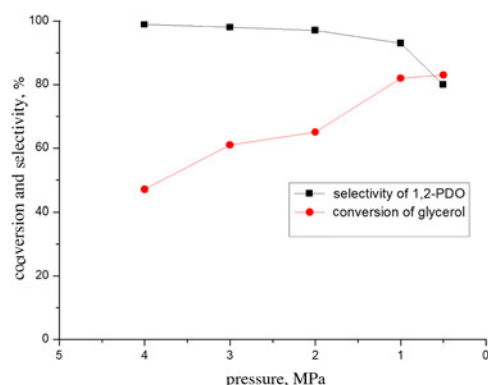


Fig. 7 Influence of hydrogen pressure on glycerol hydrogenolysis. Reaction conditions: 46 wt.% aqueous glycerol solution; H_2 /glycerol molar ratio, 35:1; and temperature, 220°C

smaller specific surface areas (see Table 2), the conversions and selectivities for 1,2-PDO using CuO/SiO_2 and $CuO-CeO_2-PTA/SiO_2$ were slightly lower. Moreover, catalytic activity further decreased when only PTA was added to the CuO/SiO_2 catalyst, giving a glycerol conversion of 88.43% and a sharply decreased 1,2-PDO selectivity of 38.36%. From the data in Table 1, we speculated that the acid strength of $CuO-PTA/SiO_2$ contributed to the decreased catalytic activity.

The effects of changing hydrogen pressure are shown in Fig. 7. Glycerol conversion dropped sharply with increasing hydrogen pressure, whereas the selectivity for 1,2-PDO slightly increased. From this, we deduced that it became more difficult for products to leave the catalyst surface as hydrogen pressure increased, causing active sites to be blocked by these products.

The effects of changing reaction temperature are shown in Fig. 8. With increasing reaction temperature, the glycerol conversion rate improved steadily, reaching 100% at 220°C. However, when the reaction temperature exceeded 220°C, the selectivity for 1,2-PDO decreased continuously due to excess glycerol hydrogenolysis, causing side reactions that produce 1-propanol, 2-propanol, and ethylene glycol (Table 3).

The effects of changing H_2 /glycerol molar ratio are shown in Fig. 9, while the influence of changing glycerol concentration is shown in Fig. 10. We found that altering both of these conditions had no significant effect on glycerol hydrogenolysis.

By optimising several reaction conditions on the continuous fixed bed reactor such as reaction temperature (220°C), H_2 pressure (0.5 MPa), H_2 /glycerol molar ratio (35:1), and glycerol concentration (100 wt.%), we achieved 100% glycerol conversion and 95%

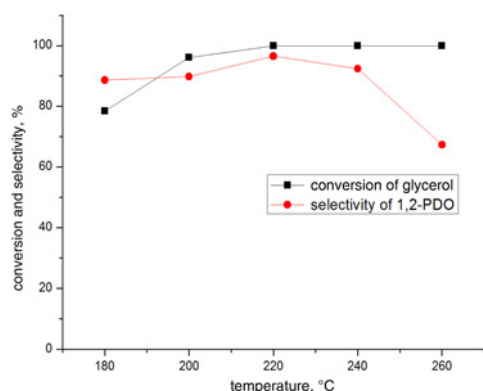


Fig. 8 Influence of temperature on glycerol hydrogenolysis. Reaction conditions: glycerol concentration, 100 wt.%; H_2 /glycerol molar ratio, 35:1; and H_2 pressure, 0.5 MPa

Table 3 Hydrogenolysis of glycerol of recycled $CuO-CeO_2/SiO_2$ catalyst

Recycles	Conversion, %	Selectivity, %
1	100.0	95.4
2	98.4	95.2
3	97.3	94.9
4	78.6	84.2

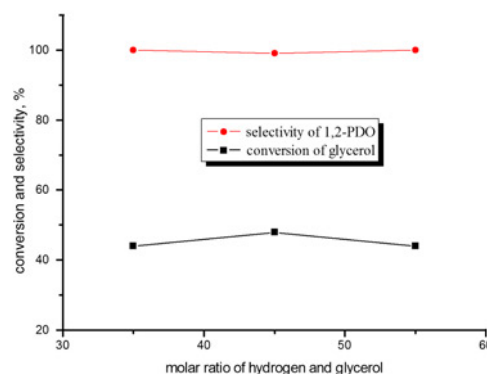


Fig. 9 Influence of H_2 /glycerol molar ratio on glycerol hydrogenolysis. Reaction conditions: glycerol concentration, 100 wt.%; H_2 pressure, 0.5 MPa; and temperature, 220°C

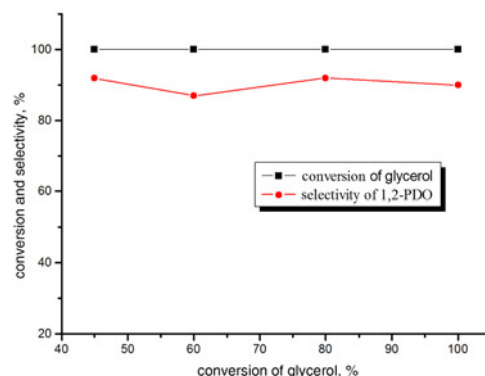


Fig. 10 Effect of glycerol concentration on glycerol hydrogenolysis. Reaction conditions: H_2 /glycerol molar ratio, 35:1; H_2 pressure, 0.5 MPa; and temperature, 220°C

selectivity for 1,2-PDO from glycerol hydrogenolysis using a modified $CuO-CeO_2/SiO_2$ catalyst. The activity of $CuO-CeO_2/SiO_2$ catalyst is higher than that of Cu/ZnO catalyst [6], and copper chromite catalysts with various promoters such as Al, Zn, and Ba [14], and hydrotalcite precursor supported Pt catalyst [17], and is comparable with that of CuO/ZnO catalysts [21].

4. Conclusions: The effects of several additives on the catalytic activity of copper-based catalysts in glycerol hydrogenolysis were investigated. In particular, the glycerol conversion rate and selectivity for 1,2-PDO were studied using CuO/SiO_2 , $CuO-PTA/SiO_2$, $CuO-CeO_2-PTA/SiO_2$, and $CuO-CeO_2/SiO_2$ as catalysts. Under a reaction temperature of 220°C, H_2 pressure of 0.5 MPa, H_2 /glycerol molar ratio of 35:1, and using a 100 wt.% aqueous glycerol solution, $CuO-CeO_2/SiO_2$ gave the highest glycerol conversion rate and outstanding selectivity for 1,2-PDO, and exhibited smaller particle sizes, better dispersion, and greater specific surface area. In comparison, $CuO-CeO_2/SiO_2$, CuO/SiO_2 , and $CuO-CeO_2-PTA/SiO_2$ had slightly lower catalytic activities

because of their smaller specific surface areas and relative instability. CuO-PTA/SiO₂ was strongly acidic, resulting in the generation of hydroxyacetone and 3-hydroxypropanol via glycerol dehydration. Dehydration and dehydrogenation of 1,2-PDO and 1,3-PDO to propanol and smaller aliphatic hydrocarbons occurred more easily due to the strong acidity of the CuO-PTA/SiO₂ catalyst, contributing to a drastic decrease in selectivity for 1,2-PDO.

5. Acknowledgments: This work was supported by grants from the National Natural Science Foundation of China (NSFC21376128), the Natural Science Foundation of Shan Dong Province (R2012BL02), and the Research Project by the Education Department of Shan Dong Province (J10LB07).

6 References

- [1] Hoekman S.K.: 'Biofuels in the U.S. – challenges and opportunities', *Renew. Energy*, 2009, **34**, (1), pp. 14–22
- [2] Manajic D., Cuzman I., Fărcaș P.: 'Renewables energies industry in the current investment context', *Timisoara J. Econ.*, 2011, **4**, (2 (14)), pp. 97–103
- [3] Huber G.W., Dumesic J.A.: 'Production of liquid alkanes by aqueous-phase processing of biomass-derived carbohydrates', *Science*, 2005, **308**, (5727), pp. 1446–1450
- [4] Song R., Qian R., Li C., *ET AL.*: 'Advances in new usage of glycerol', *China Oils Fats*, 2008, **05**, pp. 40–44
- [5] Balaraju M., Rekha V., Prasad P.S.S., *ET AL.*: 'Selective hydrogenolysis of glycerol to 1, 2 propanediol over Cu–ZnO catalysts', *Catal. Lett.*, 2008, **126**, (126), pp. 119–124
- [6] Dasari M.A., Kiatsimkul P.P., Sutterlin W.R., *ET AL.*: 'Low-pressure hydrogenolysis of glycerol to propylene glycol', *Appl. Catal. A, Gen.*, 2005, **281**, (1-2), pp. 225–231
- [7] Feng Y., Yin H., Wang A., *ET AL.*: 'Gas phase hydrogenolysis of glycerol catalyzed by Cu/ZnO/MO_x (MO_x=Al₂O₃, TiO₂, and ZrO₂) catalysts', *Midwifery*, 2011, **168**, (1), pp. 403–412
- [8] Huang L., Zhu Y., Zheng H., *ET AL.*: 'Direct conversion of glycerol into 1,3-propanediol over Cu–H₄ SiW₁₂O₄₀/SiO₂ in vapor phase', *Catal. Lett.*, 2009, **131**, (1), pp. 312–320
- [9] Schmidt S.R., Tanielyan S.K., Marin N., *ET AL.*: 'Selective conversion of glycerol to propylene glycol over fixed bed Raney[®] Cu catalysts', *Top. Catal.*, 2010, **53**, (53), pp. 1214–1216
- [10] Vasiliadou E.S., Lemonidou A.A.: 'Investigating the performance and deactivation behaviour of silica-supported copper catalysts in glycerol hydrogenolysis', *Appl. Catal. A, Gen.*, 2011, **396**, (1-2), pp. 177–185
- [11] Alhanash A., Kozhevnikova E.F., Kozhevnikov I.V.: 'Hydrogenolysis of glycerol to propanediol over Ru: polyoxometalate bifunctional catalyst', *Catal. Lett.*, 2008, **120**, (120), pp. 307–311
- [12] Feng J., Wang J., Zhou Y., *ET AL.*: 'ChemInform abstract: effect of base additives on the selective hydrogenolysis of glycerol over Ru/TiO₂ catalyst', *ChemInform*, 2008, **39**, (9), pp. 1274–1275
- [13] Vasiliadou E.S., Heracleous E., Vasalos I.A., *ET AL.*: 'Ru-based catalysts for glycerol hydrogenolysis – effect of support and metal precursor', *Appl. Catal. B, Environ.*, 2009, **92**, (1-2), pp. 90–99
- [14] Furikado I., Miyazawa T., Koso S., *ET AL.*: 'Catalytic performance of Rh/SiO₂ in glycerol reaction under hydrogen', *Green Chem.*, 2007, **9**, (6), pp. 582–588
- [15] Nakagawa Y., Tomishige K.: 'Catalyst development for the hydrogenolysis of biomass-derived chemicals to value-added ones', *Catal. Surv. Asia*, 2011, **15**, (2), pp. 111–116
- [16] Shinmi Y., Koso S., Kubota T., *ET AL.*: 'Modification of Rh/SiO₂ catalyst for the hydrogenolysis of glycerol in water', *Appl. Catal. B, Environ.*, 2010, **94**, (3), pp. 318–326
- [17] Yuan Z., Wu P., Gao J., *ET AL.*: 'Pt/solid-base: a predominant catalyst for glycerol hydrogenolysis in a base-free aqueous solution', *Catal. Lett.*, 2009, **130**, (1), pp. 261–265
- [18] Zhu S., Zhu Y., Hao S., *ET AL.*: 'Aqueous-phase hydrogenolysis of glycerol to 1,3-propanediol over Pt–H₄SiW₁₂O₄₀/SiO₂', *Catal. Lett.*, 2012, **142**, (2), pp. 267–274
- [19] Guo X., Li Y., Shi R., *ET AL.*: 'Co/MgO catalysts for hydrogenolysis of glycerol to 1, 2-propanediol', *Appl. Catal. A, Gen.*, 2009, **371**, (1), pp. 108–113
- [20] Liu Q., Guo X., Chen J., *ET AL.*: 'Cobalt nanowires prepared by heterogeneous nucleation in propanediol and their catalytic properties', *Nanotechnology*, 2008, **19**, (36), pp. 2618–2624
- [21] Nakagawa Y., Shinmi Y., Koso S., *ET AL.*: 'Direct hydrogenolysis of glycerol into 1,3-propanediol over rhenium-modified iridium catalyst', *J. Catal.*, 2010, **272**, (2), pp. 191–194
- [22] Wen G., Xu Y., Liu Q., *ET AL.*: 'Preparation of Ce-modified Raney Ni catalysts and their application in aqueous-phase reforming of cellulose', *Catal. Lett.*, 2011, **141**, (12), pp. 1851–1858
- [23] Zhou J., Zhang J., Guo X., *ET AL.*: 'Ag/Al₂O₃ for glycerol hydrogenolysis to 1,2-propanediol: activity, selectivity and deactivation', *Green Chem.*, 2012, **14**, (14), pp. 156–163